Interference Suppression Strategy for Cell-Edge Users in the Downlink

Rizwan Ghaffar, *Member, IEEE,* and Raymond Knopp, *Member, IEEE*

***Abstract*—In this paper we focus on the cell-edge users whose performance is severely limited by the interfering signals of diverse rates and strengths. In contrast to the suboptimal single-user detection, we propose an interference suppression strategy based on a low complexity matched filter (MF) based receiver. This proposed receiver exploits the structure of dominant interference in the detection process, instead of assuming it to be Gaussian and merging it in noise. This receiver is also characterized by the reduction of one complex dimension in the detection process thereby making it low complexity receiver structure. For comparison purposes, we also include the analysis of MMSE receiver and show that while MMSE detection loses one diversity order in the presence of one interferer, the proposed receiver recuperates the lost order of diversity. We further show that MMSE detection suffers from a coding loss as the interference gets stronger while the proposed receiver exhibits a coding gain as either the interference gets stronger or its modulation order decreases. Based on these results, we further propose a novel fractional frequency reuse (FFR) scheme for cellular systems.**

***Index Terms*—Interference, downlink, MMSE, max log MAP, BICM, OFDM.**

I. Introduction

To cope with the ever-increasing demands of higher spectral efficiency, spatial dimension in the form of MIMO and spectral dimension in the form of aggressive frequency reuse factor, are being incorporated in modern wireless communication systems as long term evolution (LTE), LTE-Advanced and WiMax (IEEE 802.16m). Adaptive modulation and coding schemes are being supported in the next generation wireless systems which combined with the diversified data services lead to variable transmission rate streams. These system characteristics overall effectuate an interference-limited system where one or two dominant interferences of variable rates are limiting the performance of the cell edge users. The conventional wireless systems deal with the interference either by orthogonalizing the communication links in time or frequency (*interference avoidance*) or allow the communication links to share the same degrees of freedom but leaking just enough interference to meet a desired quality of service (QoS) [1] (*interference containment*). Both of these approaches restrict the re-usability of the spectrum thereby entailing an *a priori* loss of the degrees of freedom. In the pursuit of higher spectral efficiency, modern wireless systems advocate exhaustive frequency reuse which leads to an interference-limited system especially for the cell edge users. Spatial degrees of freedom (multiple antennas) available at the users can be used to attenuate or cancel these interferences (*interference rejection*). Amongst the possible choices, linear minimum mean square error (MMSE) receiver [2] is being considered as a likely candidate for future cellular systems [3].

Multiple-antenna systems have been studied in the presence of single or multiple antenna interferences as in [4, 5] and references therein, but these interferences are assumed to be Gaussian. Recently focus has shifted on how to intelligently exploit the knowledge and/or the structure of dominant discrete interferences instead of assuming them Gaussian and merging them in noise or nulling them out. However this exploitation comes at the cost of enhanced detection complexity. The principal question in this context is, how many dominant interferences a cell-edge user is confronted with? We argue that the systematized architecture of cellular systems would restrict this number to one or two (see Fig. 1) while other interferences from relatively far cells would be weaker due to path losses. To exploit these dominant interferences, we propose a low complexity matched filter (MF) based receiver. Unlike MMSE receiver which is based on the unrealistic assumption of Gaussianity for the interferences [6], the proposed receiver considers interferences to be from discrete constellations and subsequently exploits their structure in the detection process. This MF based receiver is a low complexity adaptation of the max log MAP receiver [7] (practical version of the maximum likelihood receiver) which successfully reduces one complex dimension of the system. To the best of authors' knowledge, the result of the reduction of one complex dimension has not been known in the literature. We also show that the proposed receiver not only has full diversity but it also exhibits a coding gain (the horizontal shift of the BER curve) as either the interference gets stronger or its modulation order (rate) decreases. For comparison purposes, we also include the analysis of linear MMSE receiver which has been extensively studied in the literature both for the case of single [8] and multiple equal and unequal power interferers [9, 10]. We show again the well known result that MMSE detection loses one diversity order in the presence of one interferer [11]. In addition we show that MMSE detection, being independent of the interfering constellation, suffers from a coding loss

R. Ghaffar is with the Electrical and Computer Engineering Department, University of Waterloo, Canada e-mail: (rghaffar@uwaterloo.ca). R. Knopp is with the Mobile Communications Department, EURECOM, Sophia Antipolis, France e-mail: (raymond.knopp@eurecom.fr).

This research was supported by the European Commission under SAMURAI and IST FP7 research network of excellence NEWCOM++, as well as by EURECOM through its industrial partners Swisscom, Thales, SFR, Orange France, ST Ericsson, SAP, BMW Group, Cisco, Monaco Telecom, and Symantec.

Manuscript received October 28, 2010; revised October 10, 2011; accepted October 20, 2011.

as the interference gets stronger which is evident as MMSE detection does not exploit the interference structure in the detection process. Based on the coding gain of the proposed receiver with reference to the strength and the modulation order of the interfering stream, we further propose a novel fractional frequency reuse (FFR) scheme which is not only characterized by improved spectral efficiency but is also more energy efficient than the traditional FFR strategies.

Regarding notations, we will use lowercase or uppercase letters for scalars, lowercase boldface letters for vectors and uppercase boldface letters for matrices. $(.)^T$, $(.)^*$ and $(.)^\dagger$ indicate transpose, conjugate and conjugate transpose operations respectively. $|.|$ and $\|.\|$ indicate norm of scalar and vector. The notation $E(.)$ denotes the mathematical expectation while $Q(y) = \frac{1}{\sqrt{2\pi}} \int_y^\infty e^{-x^2/2} dx$ denotes the Gaussian Q-function. $\mathbf{A}_{M\times N}$ indicates a matrix $\mathbf{A}$ with M rows and N columns whereas $\lambda_i(\mathbf{A})$ indicates i-th eigenvalue of $\mathbf{A}$. vec $(\mathbf{A})$ denotes the vectorization operator which stacks the columns of $\mathbf{A}$ while the element at the i-th row and j-th column of matrix $\mathbf{A}$ is denoted as $\mathbf{A}(i,j)$. The matrix $\mathbf{I}_n$ is the $n \times n$ identity matrix.

The paper is divided into eight sections. In section II we define the system model while section III gives insight into the mutual information analysis of the desired stream in the presence of the interfering stream. In section IV, we give an overview of the MMSE receiver and derive the low complexity MF based receiver. Section V encompasses the pairwise error probability (PEP) analysis of these receivers which is followed by simulation results. Section VII discusses some relevant applications of interference suppression and the paper is subsequently concluded.

II. System Model

We consider the downlink of a single frequency reuse cellular system (as shown in Fig. 1) with n_r antennas at the user and the base stations (BSs) using antenna cycling [12] for transmission with each stream (codeword) being transmitted by one antenna in any dimension. Bit interleaved coded modulation (BICM) [7] because of its improved diversity over fading channels and OFDM for the reason of its associated low complexity equalization have made their ways into the ongoing wireless standardizations as LTE [13], LTE-A [14] and WiMax. We therefore assume that the BSs use BICM based OFDM system for the downlink transmission. x_1 is the symbol of the desired stream $\underline{\mathbf{x}}_1$ over a signal set $\chi_1 \subseteq \mathcal{C}$ with a Gray labeling map $\mu_1 : \{0,1\}^{\log_2|\chi_1|} \rightarrow \chi_1$ where $|\chi_1| = M_1$ is the cardinality of the constellation. x_2 is the symbol of the dominant interference stream $\underline{\mathbf{x}}_2$ over signal set χ_2 where $|\chi_2| = M_2$. Interferences from relatively distant cells are weaker and are therefore merged in noise [15].

During the transmission at BS-1, code sequence $\underline{\mathbf{c}}_1$ is interleaved by π_1 and then is mapped onto the signal sequence $\underline{\mathbf{x}}_1 \in \chi_1$. Bit interleaver for the first stream can be modeled as $\pi_1 : k^{'} \rightarrow (k,i)$ where $k^{'}$ denotes the original ordering of the coded bits $c_{k^{'}}$ of the first stream, k denotes the subcarrier index of the signal $x_{1,k}$ and i indicates the position of the bit $c_{k^{'}}$ in the symbol $x_{1,k}$. Assuming that the cyclic prefix of appropriate length is added to the OFDM symbols, transmission at the k-th frequency tone after cascading IFFT at the BS and FFT at the user is given as

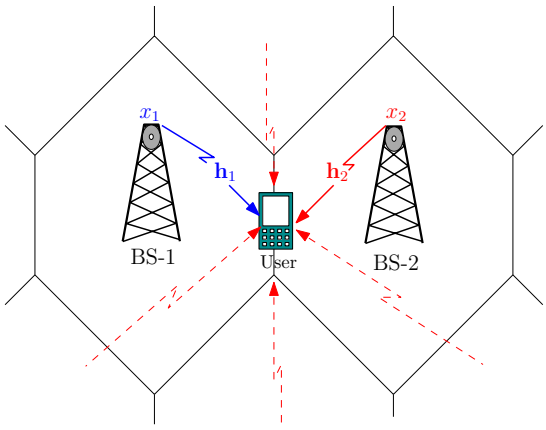

Fig. 1. Interference in cellular network. x_1 is the desired signal while x_2 is the dominant interference signal from neighboring cell. Interferences from other cells are weaker.

$$\mathbf{y}_k = \mathbf{h}_{1,k} x_{1,k} + \mathbf{h}_{2,k} x_{2,k} + \mathbf{z}_k = \mathbf{H}_k \mathbf{x}_k + \mathbf{z}_k, \quad k = 1, \cdots, T \tag{1}$$

where T is the total number of frequency tones, $\mathbf{H}_k = [\mathbf{h}_{1,k}\, \mathbf{h}_{2,k}]$ is the virtual MIMO channel from two BSs to the user at the k-th frequency tone and $\mathbf{x}_k = [x_{1,k}\, x_{2,k}]^T$. Each subcarrier corresponds to a symbol from a constellation map χ_1 for the first stream and χ_2 for the second stream. $\mathbf{y}_k, \mathbf{z}_k \in \mathbb{C}^{n_r}$ are the vectors of the received symbols and circularly symmetric complex white Gaussian noise of double-sided power spectral density $N_0/2$ at n_r receive antennas. The noise also contains weaker interferences from relatively distant BSs. $\mathbf{h}_{1,k} \in \mathbb{C}^{n_r}$ is the vector characterizing flat fading channel response from the first BS to n_r receive antennas at the k-th subcarrier. The complex symbols $x_{1,k}$ and $x_{2,k}$ of two streams are assumed to be independent with variances σ_1^2 and σ_2^2 respectively. The channels at different subcarriers are also assumed to be independent. For spatial correlation, we consider *Kronecker correlation model*, i.e.

$$\mathbf{H}_k = \mathbf{\Psi}_R^{1/2} \mathbf{W}_k \mathbf{\Psi}_T^{1/2} \tag{2}$$

where $\mathbf{W}_k$ is the spatially white (Rayleigh iid) MIMO channel. $\mathbf{\Psi}_R$ is the $n_r \times n_r$ receive while $\mathbf{\Psi}_T$ is the 2×2 transmit correlation matrix between two BSs. This correlation model also known as doubly correlated channel model where correlation is in the product form of transmit and receive correlation was verified and analyzed in several investigations (see e.g. [16–21]). For the structure of the correlation, we consider a simple single-parameter exponential correlation matrix model [22].

III. An Information-Theoretic View

To outline the significance of the strength and the modulation order of dominant interference in the detection of desired stream, we focus on the mutual information analysis. Here we do not resort to the simplifying Gaussian assumption for the interference but consider it to be discrete belonging to a finite QAM constellation. Assuming perfect CSI at the

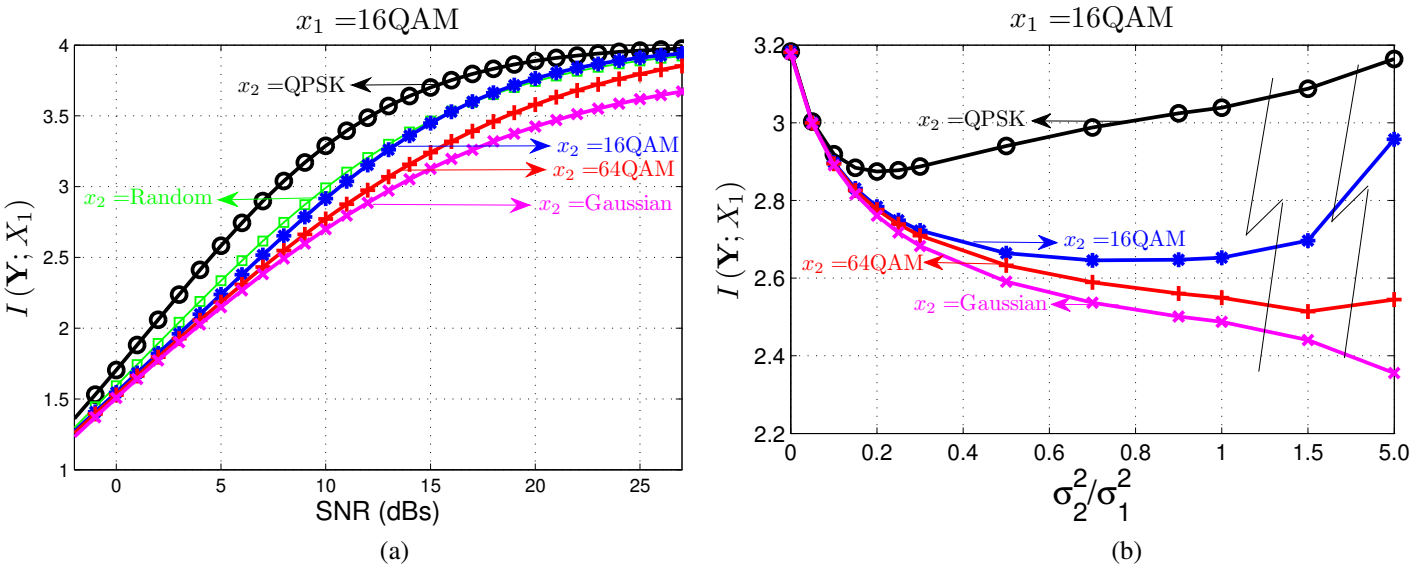

Fig. 2. Mutual information of the desired stream x_1 =16QAM in the presence of interference stream x_2 for different constellations. In Fig. (a), interference is of the same strength as the desired stream, i.e. $\sigma_2^2/\sigma_1^2 = 1$ whereas in Fig. (b), the strength of interference stream relative to the desired stream, i.e. σ_2^2/σ_1^2 is varied while SNR is fixed to 11dB. Note that random interference refers to the case when interference is not static but changes randomly between QPSK, 16QAM and 64QAM.

receiver (user) and dropping the frequency index for notational convenience, the conditional mutual information (for a given channel realization) of desired stream is given as

$$I(\mathbf{Y};X_1|\mathbf{H}=\mathbb{H}) = \mathcal{H}(X_1|\mathbf{H}=\mathbb{H}) - \mathcal{H}(X_1|\mathbf{Y},\mathbf{H}=\mathbb{H})$$
$$= \log M_1 - \frac{1}{M_1 M_2}\sum_{x_1}\sum_{x_2}\int_{\mathbf{y}} p(\mathbf{y}|x_1,x_2,\mathbf{H}=\mathbb{H})$$
$$\times \log \frac{\sum_{x_1'}\sum_{x_2'} p\left(\mathbf{y}|x_1',x_2',\mathbf{H}=\mathbb{H}\right)}{\sum_{x_2'} p\left(\mathbf{y}|x_1,x_2',\mathbf{H}=\mathbb{H}\right)} d\mathbf{y} \quad (3)$$

Note that $x_1' \in \chi_1$ and $x_2' \in \chi_2$. $p(\mathbf{y}|x_1,x_2,\mathbf{H}=\mathbb{H})$ for a given channel realization is the probability of Gaussian noise, i.e. $p(\mathbf{z})$, so (3) can be approximated numerically using sampling (Monte-Carlo) methods with N_z realizations of the noise, i.e.

$$I(\mathbf{Y};X_1|\mathbf{H}=\mathbb{H}) = \log M_1 - \frac{1}{M_1 M_2 N_z}$$
$$\times\left(\sum_{x_1}\sum_{x_2}\sum_{\mathbf{z}}^{N_z}\log\frac{\sum_{x_1'}\sum_{x_2'}\exp\left[-\frac{1}{N_0}\left\|\mathbf{y}-\mathbf{h}_1x_1'-\mathbf{h}_2x_2'\right\|^2\right]}{\sum_{x_2'}\exp\left[-\frac{1}{N_0}\left\|\mathbf{y}-\mathbf{h}_1x_1-\mathbf{h}_2x_2'\right\|^2\right]}\right) \quad (4)$$

Averaging over channel leads to

$$I(\mathbf{Y};X_1|\mathbf{H}) = \mathbb{E}_{\mathbf{H}}\left[I(\mathbf{Y};X_1|\mathbf{H}=\mathbb{H})\right] \quad (5)$$

For comparison purposes, we consider the case when the desired stream x_1 belongs to finite alphabet ($x_1 \in M_1$) but the interference stream is Gaussian. Estimation of the conditional mutual information of the desired stream using Monte-Carlo simulations is given as

$$I(\mathbf{Y};X_1|\mathbf{H}=\mathbb{H}) = \log M_1 - \frac{1}{M_1 N_z}$$
$$\times\left(\sum_{x_1}\sum_{\mathbf{z}}^{N_z}\log\frac{\sum_{x_1'}\exp\left\{-\left[\mathbf{y}-\mathbf{h}_1x_1'\right]^\dagger\left(\sigma_2^2\mathbf{h}_2\mathbf{h}_2^\dagger+N_0\mathbf{I}\right)^{-1}\left[\mathbf{y}-\mathbf{h}_1x_1'\right]\right\}}{\exp\left\{-\left[\mathbf{y}-\mathbf{h}_1x_1\right]^\dagger\left(\sigma_2^2\mathbf{h}_2\mathbf{h}_2^\dagger+N_0\mathbf{I}\right)^{-1}\left[\mathbf{y}-\mathbf{h}_1x_1\right]\right\}}\right)$$

To segregate the effects of the modulation order and the strength of the interference on the mutual information of the desired stream, we carry out two sets of simulations. Fig. 2(a) shows the effects of the modulation order (constellation size) of the interference stream on the mutual information of the desired stream where the strength of the interfering stream is kept constant. It clearly illustrates that there is a significant boost in the mutual information of the desired stream when the interference stream is from discrete alphabets as compared to the case when it belongs to Gaussian alphabets. Gaussian alphabets are indeed entropy maximizers [23] but the same is not true for Gaussian interference. Discrete interference possesses the structure that can be exploited in the detection process however if the interference is Gaussian, it is void of any structure and therefore can not facilitate the detection of the desired stream. Note that the gap between the mutual information of Gaussian and discrete interference shrinks as the constellation size of the interference stream increases. This diminution of gap is related to the proximity of the behavior of larger constellation interference to Gaussianity as both are characterized by high peak to average power ratios. We have also considered the case of random interference which may arise due to different multi-user allocations in the interfering cell.

Fig. 2(b) shows the effect of the strength of the interference on the mutual information of the desired stream when SNR (of the desired stream) is kept constant. For the case of interference belonging to discrete alphabets, the mutual information of the desired stream first declines and then increases as the interference gets stronger. This point of transformation depends on the relative strength and the constellation size of the interference stream to that of the desired stream. As the strength of interference relative to the SNR allows its partial decoding, the mutual information

of the desired stream starts improving with the interference strength. So as interference gets stronger, its structure can be more effectively exploited thereby improving the mutual information of the desired stream. However contrary is the case for Gaussian interference where the mutual information of the desired stream decreases as the interference stream gets stronger. This analysis underlines the inevitability of a receiver which is adept in exploiting the structure of interference in the detection process instead of assuming it to be Gaussian.

IV. RECEIVERS

Though our focus in this paper is on the case of one dominant interferer, we consider the general case where the user faces $(n-1)$ interferences from $(n-1)$ BSs. Without loss of generality, we assume that stream 1 is the desired stream where the term 'stream' means the codeword transmitted by the BS.

A. Low complexity MF based receiver

For maximum likelihood (ML) soft detection of x_1, the receiver calculates log-likelihood ratios (LLRs) for all the bits that constitute x_1 by summing the Euclidean distances for the values of $x_1, \cdots, x_n$ for which that particular bit of x_1 is one and zero thereby amounting to $2^{(|\chi_1|\cdots|\chi_n|)}$ terms. In many cases of practical interest, one resorts to the approximation of replacing the sums with the largest term which is equivalent to minimizing the Euclidean distance and is termed as max log MAP approach [7]. LLR of a bit is the difference of two bit metrics where that particular bit is one and zero respectively. The max log MAP bit metric for the bit $c_{k'}$ on the first stream (desired stream) at the k-th subcarrier is given as [24]

$$\Lambda_1^i\left(\mathbf{y}_k, c_{k'}\right) \approx \min_{x_1 \in \chi^i_{1,c_{k'}}, x_2 \in \chi_2, \cdots, x_n \in \chi_n} \left\|\mathbf{y}_k - \mathbf{h}_{1,k}x_1 - \cdots - \mathbf{h}_{n,k}x_n\right\|^2 \tag{6}$$

where $\chi^i_{1,c_{k'}}$ denotes the subset of the signal set $x_1 \in \chi_1$ whose labels have the value $c_{k'} \in \{0,1\}$ in the position i. As the minimization in (6) involves a search over all constellation points of interferences and half the constellation points of the desired stream, so it has a computational complexity in the order of $\mathcal{O}\left(|\chi_1|\cdots|\chi_n|\right)$. Expanding further the bit metric and grouping the terms containing x_n, we get

$$\begin{aligned}\Lambda_1^i\left(\mathbf{y}_k, c_{k'}\right) \approx \min_{x_1 \in \chi^i_{1,c_{k'}}, x_2 \in \chi_2, \cdots, x_n \in \chi_n} \Bigg\{ & \left\|\mathbf{y}_k\right\|^2 + \sum_{j=1}^{n-1}\left\|\mathbf{h}_{j,k}x_j\right\|^2 \\ & + 2\sum_{j=1}^{n-1}\sum_{l=j+1}^{n-1}\left(p_{jl,k}x_j^* x_l\right)_R - 2\sum_{j=1}^{n-1}\left(y_{j,k}x_j^*\right)_R \\ & + 2\sum_{j=1}^{n-1}\left(p_{jn,k}x_j^* x_n\right)_R - 2\left(y_{n,k}x_n^*\right)_R + \left\|\mathbf{h}_{n,k}x_n\right\|^2 \Bigg\}\end{aligned}$$

where $y_{j,k} = \mathbf{h}_{j,k}^\dagger \mathbf{y}_k$ is the MF output for the j-th BS and $p_{jl,k} = \mathbf{h}_{j,k}^\dagger \mathbf{h}_{l,k}$ is the cross correlation between the channels of the j-th and l-th BSs at the k-th subcarrier. Breaking some of the terms in their real and imaginary parts, we have

$$\begin{aligned}\Lambda_1^i\left(\mathbf{y}_k, c_{k'}\right) \approx \min_{x_1 \in \chi^i_{1,c_{k'}} \cdots x_n \in \chi_n} \Bigg\{ & \sum_{j=1}^{n-1}\left\|\mathbf{h}_{j,k}x_j\right\|^2 + 2\sum_{j=1}^{n-1}\sum_{l=j+1}^{n-1}\left(p_{jl,k}x_j^* x_l\right)_R \\ & - 2\sum_{j=1}^{n-1}\left(y_{j,k}x_j^*\right)_R + \left\|\mathbf{h}_{n,k}\right\|^2 x_{n,R}^2 + \left\|\mathbf{h}_{n,k}\right\|^2 x_{n,I}^2 \\ & + 2\left(\sum_{j=1}^{n-1}\left(p_{jn,k,R}x_{j,R} + p_{jn,k,I}x_{j,I}\right) - y_{n,k,R}\right)x_{n,R} \\ & + 2\left(\sum_{j=1}^{n-1}\left(p_{jn,k,R}x_{j,I} - p_{jn,k,I}x_{j,R}\right) - y_{n,k,I}\right)x_{n,I} \Bigg\}\end{aligned} \tag{7}$$

where subscripts $(a)_R$ or a_R indicate the real part and $(a)_I$ or a_I indicate the imaginary part of a. For x_n belonging to the equal energy alphabets, the value of its real part $x_{n,R}$ and its imaginary part $x_{n,I}$ which minimize (7) need to be in the opposite directions of their multiplicative factors, i.e. $\left(\sum_{j=1}^{n-1}\left(p_{jn,k,R}x_{j,R} + p_{jn,k,I}x_{j,I}\right) - y_{n,k,R}\right)$ and $\left(\sum_{j=1}^{n-1}\left(p_{jn,k,R}x_{j,I} - p_{jn,k,I}x_{j,R}\right) - y_{n,k,I}\right)$ respectively thereby evading the search on $|\chi_n|$ constellations points of x_n and reducing one complex dimension of the system, i.e.

$$\begin{aligned}\Lambda_1^i\left(\mathbf{y}_k, c_{k'}\right) \approx \min_{x_1 \in \chi^i_{1,c_{k'}}, \cdots, x_{n-1} \in \chi_{n-1}} \Bigg\{ & \sum_{j=1}^{n-1}\left\|\mathbf{h}_{j,k}x_j\right\|^2 \\ & + 2\sum_{j=1}^{n-1}\sum_{l=j+1}^{n-1}\left(p_{jl,k}x_j^* x_l\right)_R - 2\sum_{j=1}^{n-1}\left(y_{j,k}x_j^*\right)_R \\ & - 2\left|\sum_{j=1}^{n-1}\left(p_{jn,k,R}x_{j,R} + p_{jn,k,I}x_{j,I}\right) - y_{n,k,R}\right|\left|x_{n,R}\right| \\ & - 2\left|\sum_{j=1}^{n-1}\left(p_{jn,k,R}x_{j,I} - p_{jn,k,I}x_{j,R}\right) - y_{n,k,I}\right|\left|x_{n,I}\right| \Bigg\}\end{aligned}$$

For x_n belonging to non-equal energy alphabets, the problem of finding $x_{n,R}$ and $x_{n,I}$ which minimize (7) is the minimization problem of a quadratic function and these are given as

$$\begin{aligned} x_{n,R} &\rightarrow -\frac{\sum_{j=1}^{n-1}\left(p_{jn,k,R}x_{j,R} + p_{jn,k,I}x_{j,I}\right) - y_{n,k,R}}{\left\|\mathbf{h}_{n,k}\right\|^2} \\ x_{n,I} &\rightarrow -\frac{\sum_{j=1}^{n-1}\left(p_{jn,k,R}x_{j,I} - p_{jn,k,I}x_{j,R}\right) - y_{n,k,I}}{\left\|\mathbf{h}_{n,k}\right\|^2} \end{aligned} \tag{8}$$

where $\rightarrow$ indicates the quantization process in which amongst the finite available points, the point closest to the calculated continuous value is selected, i.e. if x_n belongs to 64QAM, then instead of searching 64 constellation points for the minimization of (7), the metric (8) reduces it to merely 2 operations thereby trimming down one complex dimension. This bit metric implies the reduction in complexity to $\mathcal{O}\left(|\chi_1|\cdots|\chi_{n-1}|\right)$. Note that this result is also valid for the general multi-stream (spatially multiplexed) single-user MIMO systems. The reduction of one complex dimension without any additional processing is a fundamental result for lower dimensional systems. Additionally this bit metric being based on the MF outputs and channel correlations implies straightforward hardware implementation. The intricacy in the practical implementation of a higher dimensional MIMO system due to space (requisite antenna spacing) and technology

constraints underlines the significance of complexity reduction algorithms for lower dimensional systems.

The prerequisites of the proposed receiver are the knowledge of interference channel and its constellation. Moreover BSs need to be synchronized in time division duplex (TDD) mode however this constraint is not compelling in frequency division duplex (FDD) mode. Transmission of orthogonal pilot signals by the neighboring BSs is a requisite to enable the users to estimate the interference channels. As an example, we consider how these prerequisites can be met in 3GPP LTE. The orthogonality among pilot signals can be achieved as 3GPP LTE considers three non-overlapping formats of pilot signals [13]. However these pilot signals of the neighboring BS would interfere with the control information or data of the desired BS. The downlink control information (DCI) is heavily protected (coded) [13] so user after decoding its control information can strip it off thereby leading to clean pilot signals of the interfering BS. As the DCI in 3GPP LTE does not include the information of interfering constellation, we shall later discuss (Sec VI) a MF based blind receiver which is unaware of the knowledge of the constellation of interference.

B. Linear MMSE receiver

The linear MMSE filter to detect first stream is given by

$$\mathbf{f}_{1,k} = \left(\mathbf{h}_{1,k}^{\dagger}\mathbf{R}_{2,k}^{-1}\mathbf{h}_{1,k} + \sigma_1^{-2}\right)^{-1}\mathbf{R}_{2,k}^{-1}\mathbf{h}_{1,k}$$

where $\mathbf{R}_{2,k} = \sum_{l=2}^{n}\sigma_l^2\mathbf{h}_{l,k}\mathbf{h}_{l,k}^{\dagger} + N_0\mathbf{I}$. After the application of MMSE filter, we get

$$y_k = \mathbf{f}_{1,k}^{\dagger}\mathbf{y}_k = \alpha_k x_{1,k} + z_k$$

where $\alpha_k = \mathbf{f}_{1,k}^{\dagger}\mathbf{h}_{1,k}$ and z_k is assumed to be zero mean complex Gaussian random variable with variance $N_k = \mathbf{f}_{1,k}^{\dagger}\mathbf{R}_{2,k}\mathbf{f}_{1,k}$. Gaussianity has been assumed for the post detection interference which increases the sub-optimality of MMSE, notably in the case of less number of interferers [25].

V. PEP Analysis

In this section we carry out the PEP analysis of the proposed low complexity MF based receiver [26] and MMSE receiver for the case of one dominant interferer.

A. Low complexity MF based receiver

The PEP between correct codeword $\underline{\mathbf{c}}_1$ and error codeword $\hat{\underline{\mathbf{c}}}_1$, i.e. $P\left(\underline{\mathbf{c}}_1 \rightarrow \hat{\underline{\mathbf{c}}}_1\right) = \mathcal{P}_{\underline{\mathbf{c}}_1}^{\hat{\underline{\mathbf{c}}}_1}$ has been derived in Appendix A and is given as

$$\mathcal{P}_{\underline{\mathbf{c}}_1}^{\hat{\underline{\mathbf{c}}}_1} \leq \frac{1}{2}\left(\frac{4N_0}{\sigma_1^2\breve{d}_{1,\min}^2}\right)^{\kappa d_{free}}\left(\prod_{l=1}^{\kappa}\frac{1}{\left(\lambda_l\left(\mathbf{\Psi}_R\right)\right)^{d_{free}}}\right)\left(\frac{1}{[\theta]^{d_{free}}}\right)^{\kappa} \times\left(\sum_{j=0}^{d_{free}}\mathrm{C}_j^{d_{free}}\frac{\left(P\left(\hat{x}_{2,k}\neq x_{2,k}\right)\right)^j\left(1-P\left(\hat{x}_{2,k}\neq x_{2,k}\right)\right)^{d_{free}-j}}{\left(1+\frac{\sigma_2^2\breve{d}_{2,\min}^2}{\sigma_1^2\breve{d}_{1,\min}^2}\right)^{j\kappa}}\right) \tag{9}$$

where $d_{j,\min}^2 = \sigma_j^2\breve{d}_{j,\min}^2$ with $\breve{d}_{j,\min}^2$ being the normalized minimum distance of the constellation χ_j for $j = \{1,2\}$ and $\kappa = \mathrm{rank}\left(\mathbf{\Psi}_R\right)$. d_{free} is the minimum Hamming distance of the code. $[\theta]^{d_{free}}$ indicates the product $\theta_1\theta_2\cdots\theta_{d_{free}}$ where θs are related to the eigenvalues of the transmit correlation matrix and are given by (15) in Appendix A. $\mathrm{C}_j^{d_{free}}$ is the binomial coefficient while $P\left(\hat{x}_{2,k}\neq x_{2,k}\right)$ is the uncoded probability that the output of max log MAP detector $\hat{x}_{2,k}$ is not equal to the actual transmitted symbol $x_{2,k}$ and has been derived in Appendix C. Note that for the case of no transmit but only receive correlation, the PEP is upper bounded as

$$\mathcal{P}_{\underline{\mathbf{c}}_1}^{\hat{\underline{\mathbf{c}}}_1} \leq \frac{1}{2}\left(\frac{4N_0}{\sigma_1^2\breve{d}_{1,\min}^2}\right)^{\kappa d_{free}}\left(\prod_{l=1}^{\kappa}\frac{1}{\left(\lambda_l\left(\mathbf{\Psi}_R\right)\right)^{d_{free}}}\right) \times\left(\sum_{j=0}^{d_{free}}\mathrm{C}_j^{d_{free}}\frac{\left(P\left(\hat{x}_{2,k}\neq x_{2,k}\right)\right)^j\left(1-P\left(\hat{x}_{2,k}\neq x_{2,k}\right)\right)^{d_{free}-j}}{\left(1+\frac{\sigma_2^2\breve{d}_{2,\min}^2}{\sigma_1^2\breve{d}_{1,\min}^2}\right)^{j\kappa}}\right)$$

while for the case of iid fading, PEP is upper bounded as

$$\mathcal{P}_{\underline{\mathbf{c}}_1}^{\hat{\underline{\mathbf{c}}}_1} \leq \frac{1}{2}\left(\frac{4N_0}{\sigma_1^2\breve{d}_{1,\min}^2}\right)^{n_r d_{free}} \times\left(\sum_{j=0}^{d_{free}}\mathrm{C}_j^{d_{free}}\frac{\left(P\left(\hat{x}_{2,k}\neq x_{2,k}\right)\right)^j\left(1-P\left(\hat{x}_{2,k}\neq x_{2,k}\right)\right)^{d_{free}-j}}{\left(1+\frac{\sigma_2^2\breve{d}_{2,\min}^2}{\sigma_1^2\breve{d}_{1,\min}^2}\right)^{jn_r}}\right)$$

These expressions show that the MF based receiver achieves full diversity of the system, i.e. κd_{free} which increases to $n_r d_{free}$ when $\mathbf{\Psi}_R$ is full rank. The rank of the receive correlation matrix affects the diversity order while the eigenvalues of the transmit and receive correlation matrices affect the coding gain. Another interesting result is that the coding gain of MF based receiver increases as the interference gets stronger relative to the desired stream, i.e. $\sigma_2^2 > \sigma_1^2$ or the modulation order/constellation size of interference decreases relative to the desired stream, i.e. $\breve{d}_{2,\min}^2 > \breve{d}_{1,\min}^2$.

B. PEP Analysis - MMSE receiver

PEP for MMSE receiver for the case of receive correlation matrix to be full rank has been derived in Appendix B and is given as

$$\mathcal{P}_{\underline{\mathbf{c}}_1}^{\hat{\underline{\mathbf{c}}}_1} \leq \frac{1}{2}\left(\frac{4N_0}{\sigma_1^2\breve{d}_{1,\min}^2}\right)^{d_{free}(n_r-1)}\left(\frac{4}{\sigma_1^2\breve{d}_{1,\min}^2}\right)^{d_{free}} \times \left(n_r\sigma_2^2+N_0\right)^{d_{free}}\prod_{i=1}^{n_r}\frac{1}{\lambda_i\left(\mathbf{\Psi}_R\right)^{d_{free}}} \tag{10}$$

thereby indicating the diversity order of $d_{free}\left(n_r-1\right)$. (10) not only demonstrates the well known result of the loss of one diversity order in MMSE detection in the presence of one interferer [27] but also exhibits a coding loss as the interference gets stronger which is contrary to the case of MF based receiver. Interestingly, the performance of MMSE receiver is not dependent on the modulation order of interference which is again divergent from the MF based receiver.

VI. Simulation Results

We carry out three sets of simulations and compare the performance of low complexity MF based receiver and linear

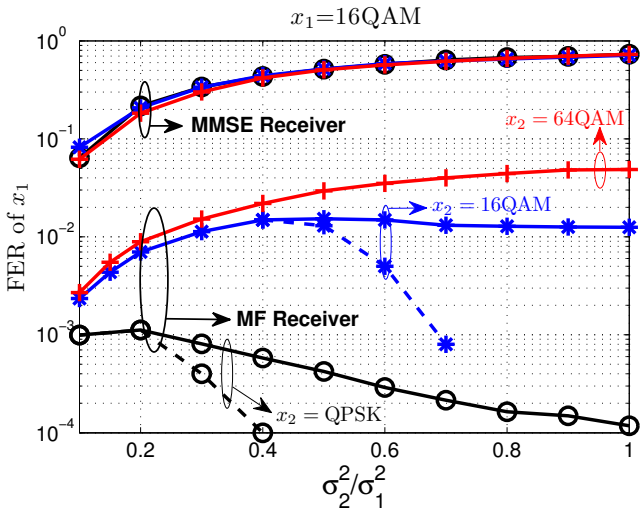

Fig. 3. Effect of interference strength. Desired stream x_1 is 16QAM while interference stream x_2 is QPSK, 16QAM and 64QAM. Amongst the curves of MF based receiver, dashed lines indicate SIC based detection. 64 state, rate-$1/2$ convolutional code is used while the SNR is 11 dB.

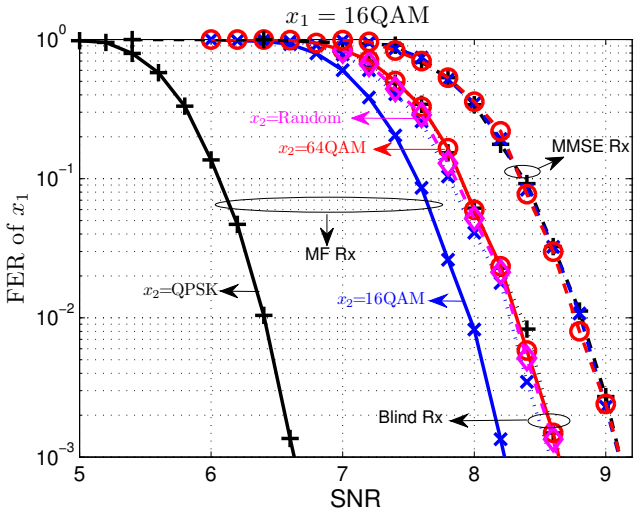

Fig. 4. Effect of the knowledge of interfering constellation. Continuous lines indicate the case when user has the knowledge of interfering constellation and the detection is done by MF based receiver (MF Rx) while dotted lines indicate the case when user does not have this knowledge and assumes the interference to be from 64QAM (Blind Rx). Dashed lines indicate detection by MMSE receiver (MMSE Rx). The case of random interference is also considered where interference is randomly generated from QPSK, 16QAM and 64QAM. Note that $\sigma_2^2/\sigma_1^2 = 1$. LTE turbo code (rate $1/2$) is used with maximum of 5 decoding iterations using max log MAP decoder.

MMSE receiver. In the first set of simulations, we consider the effects of the strength and the modulation order of interference on both the receivers while second set reflects on the significance of the knowledge of interfering constellation for the MF based receiver. Third set considers realistic channel models and shows the degrading effects of spatial and spectral correlation on both receiver structures. In the simulation setup, we consider 2 BSs, each using BICM OFDM system for downlink transmission using the *de facto* standard, 64 state $(133, 171)$ rate-$1/2$ convolutional encoder of 802.11n standard or the punctured rate $1/2$ turbo code[1] of 3GPP LTE [13]. For the first two sets of simulations, we consider an ideal OFDM based system (no ISI) with fully interleaved channel while for the third set, we consider realistic 3GPP LTE channel models [28]. We assume antenna cycling at the BS and receive diversity at the user with two antennas. We assume perfect channel state information (CSI) at the user and no CSI at the BSs. Furthermore, all mappings of the coded bits to QAM symbols use Gray encoding. In the simulations, we look at the frame error rates (FER) of the desired stream with the frame length of 1056 information bits.

To segregate the effects of the strength and the modulation order of interference stream in the first set of simulations, SNR (of desired stream) is kept constant as interference gets stronger while the channel is considered to have iid Gaussian matrix entries. Fig. 3 shows the simulated FERs of the desired stream. These results show that the performance of MMSE detection is independent of the modulation order of the interference stream but its dependence on interference strength is considerable. The performance substantially degrades as the interferer gets stronger. Contrary is the case for the low complexity MF based receiver, where a significant improvement is observed in the performance as the interference gets stronger especially when interference has a lower modulation order as compared to the desired stream. In such a case, we have also considered successive interference cancellation (SIC) based detection, i.e. when interference strength allows its detection, user first detects interference by the MF based receiver, strips it out and then detects the desired stream. In the case when interference has a higher modulation order as compared to the desired stream, the performance of MF based receiver would improve when the interference stream is substantially stronger than the desired stream, a case unlikely to occur in the cellular scenario due to handover algorithms. Improvement in the performance of MF based receiver as interference gets stronger is attributed to the partial decoding of the interference [29]. It is also observed that for a given interference level, the performance is generally degraded as the modulation order of the interfering stream increases. The performance gap with respect to the MMSE receiver decreases as the desired and the interference streams grow in the constellation sizes. This trend can be attributed to the proximity of the behavior of these larger constellations to Gaussianity due to their high peak to average power ratio and further to the optimality of MMSE detection for Gaussian alphabets.

MF based receiver needs knowledge of the interfering constellation and the transmission of this information entails signaling overhead. In the second set of simulations, we look at the significance of this information by considering two cases, i.e. when the user has knowledge of interfering constellation and when the user does not have this knowledge. For the latter case, user assumes interference from 64QAM, i.e. the highest possible modulation order in LTE and LTE-Advanced and the corresponding results are shown in Fig. 4. To avoid congested figure, we have not shown the results

[1]The LTE turbo decoder design was performed using the coded modulation library www.iterativesolutions.com

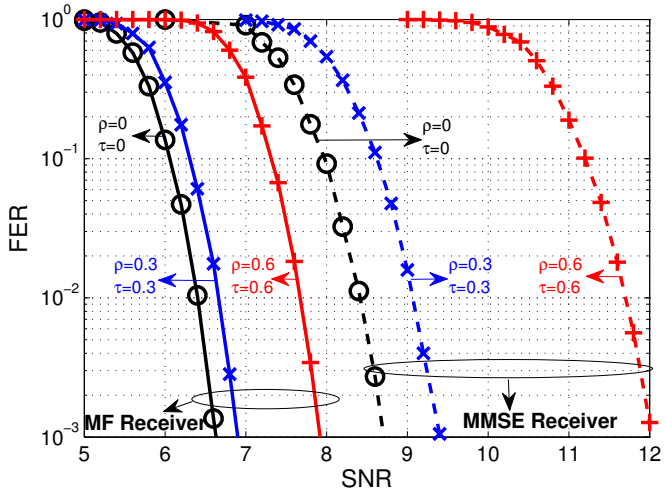

Fig. 5. Effect of spatial correlation. Desired stream x_1 is 16QAM while interference stream x_2 is QPSK. Continuous lines indicate low complexity MF based receiver while dashed lines indicate linear MMSE receiver. LTE turbo code (rate $1/2$) is used with maximum of 5 decoding iterations using max log MAP decoder. ρ and τ are the receive and transmit correlation parameters as per exponential correlation model [22].

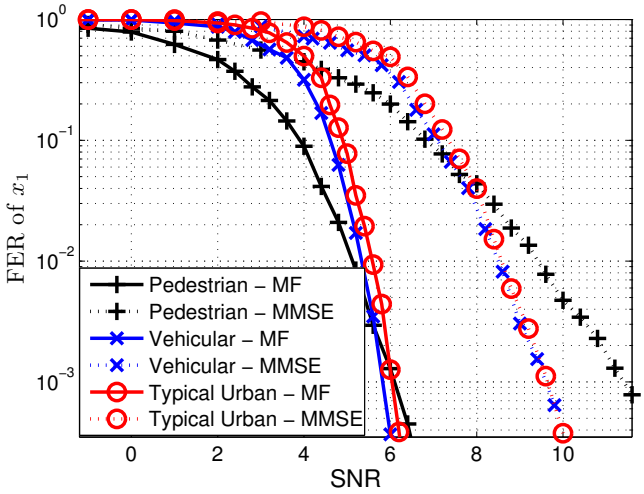

Fig. 6. Effect of spectral correlation. 3GPP LTE channel models [28] are considered. The subcarrier spacing is 15KHz and the bandwidth is 20MHz as per 3GPP LTE. Desired stream x_1 is 16QAM while interference stream x_2 is QPSK. Continuous lines indicate detection by MF based receiver while dashed lines indicate linear MMSE detection. LTE turbo code (rate $1/2$) is used with maximum of 5 decoding iterations using max log MAP decoder.

for assuming unknown interference to be QPSK or 16QAM which in fact lead to much degraded performance. This is attributed to the fact that assuming unknown interference to be from a higher order modulation amongst the possible modulation alphabets includes the lower modulation orders as special cases (with proper scaling), however the converse is not true. Note that the gains of exploiting the structure of lower modulation order interference can not be realized once the interfering constellation is not known. Assuming interference to be 64QAM once it actually belongs to QPSK constellation leads to approximately the same performance once the interference is actually from 64QAM. In a more realistic scenario, the allocation of subcarriers to the users in the neighboring cell may not coincide with the subcarrier allocation to users in the cell under consideration thereby resulting into different interfering constellations on different subcarriers. To take this into account, we have considered the case of non-static interference which is randomly generated from QPSK, 16QAM and 64QAM constellations and the user assumes this random interference to be from 64QAM. Performance curves for assuming interference to be from 64QAM (dotted lines) once the interference is actually from QPSK, 16QAM, 64QAM and random are very close to each other. This assumption is therefore a suitable compromise though the gains of exploiting lower modulation order interference can only be realized once the users have knowledge of interfering constellation. This analysis motivates the information of interfering constellation to be included in the control information in future wireless systems as ongoing standardization of LTE-Advanced [30].

Third set of simulations looks at the degrading effects of spatial and spectral correlation. For the structure of the spatial correlation matrix, we have considered exponential correlation matrix model [22] and the results are shown in Fig. 5. To study the effect of spectral correlation, we have considered 3GPP LTE channel model introduced in [28] for three representative scenarios, i.e. pedestrian, vehicular and typical urban scenario and the results are shown in Fig. 6. The transmission chain is dominantly LTE compliant with 15KHz subcarrier-spacing and 20 MHz system bandwidth. The results show that the degrading effect of spatial and spectral correlation is more pronounced for MMSE receiver as compared to the case of MF based receiver as the SNR gap between the performance of MMSE receiver and MF based receiver increases once there is spatial or spectral correlation in the channel. As there is less frequency diversity in the channel for the pedestrian scenario, the performance of MMSE detection is further degraded. Note that we have not plotted the upper bounds of error probability in these simulation results to avoid congested figures. These PEP bounds in fact give us an understanding of the behavior of the desired stream in the presence of interference stream under different scenarios and the simulation results have verified the findings of PEP analysis.

VII. Novel Fractional Frequency Reuse Scheme

FFR has mainly been discussed in the cellular network standardization as 3GPP and 3GPP2 [31] with the objective of *interference avoidance* for the cell-edge users as shown in Fig. 7a. By splitting the given bandwidth into an inner and an outer part and their subsequent allocation to *near* and *far* users with different powers and frequency reuse factors, it targets *zero interference* and subsequently low complexity single-user detection for cell-edge users. In this section, we contest this idea and propose a novel FFR scheme (Fig. 7b) with enhanced spectral efficiency showing that by allowing limited interference, we can still achieve the objective of low complexity detection by employing earlier proposed MF based receiver. Frequency reuse factor for the cell-edge users

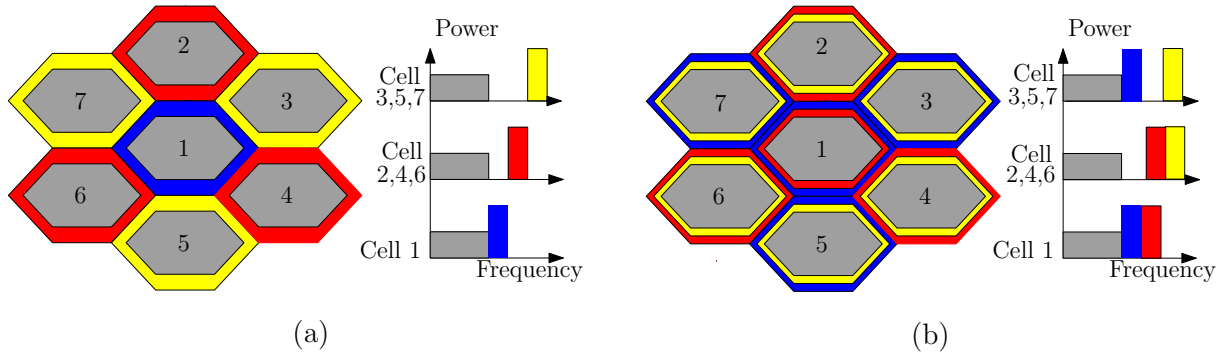

Fig. 7. Existing and proposed FFR in LTE. In Fig. (a), i.e. existing FFR, the frequency reuse factor for cell edge users is 3 whereas in Fig. (b), i.e. proposed FFR, the frequency reuse factor for cell edge users is 1.5.

TABLE I
THE PERCENTAGE DIFFERENCE: $(P_u - P_{nu})/P_u$ BETWEEN NONUNIFORM RATE STREAMS AND UNIFORM RATE STREAMS. HERE 3GPP RATE $1/2$ TURBO CODE IS USED.

Cell Edge Users		Uniform	Nonuniform	Efficiency
Cell 1	Cell 2	$P_u = \frac{\sigma_1^2}{N_0} + \frac{\sigma_2^2}{N_0}$	$P_{nu} = \frac{\sigma_1^2}{N_0} + \frac{\sigma_2^2}{N_0}$	%
User 1=3bps/Hz, User 2=1bps/Hz	User 1=3bps/Hz, User 2=1bps/Hz	50.94+2.59	18.62+18.62	30.43%
User 1=2bps/Hz, User 2=1bps/Hz	User 1=2bps/Hz, User 2=1bps/Hz	12.47+2.59	6.37+6.37	15.41%
User 1=3bps/Hz, User 2=2bps/Hz	User 1=3bps/Hz, User 2=2bps/Hz	50.94+12.47	28.94+28.94	8.72%

reduces from 3 to 1.5 [32] thereby improving the spectral efficiency. The modulation order or rate of this out-of-cell interference can be managed to allow its effective exploitation in the detection process which further improves the energy efficiency of the network. To achieve this, subcarrier allocation is combined with the rate allocation to take advantage of the effective exploitation of relatively lower rate interference in the detection process. This exploitation leads to the reduction of the required SNR at the user while ensuring a predefined QoS which subsequently leads to the minimization of the transmit power at the BSs.

To illustrate the energy savings by the exploitation of lower rate interference, we consider the effects of different rates of interference on the detection by the MF based receiver as shown in Fig. 8. The simulation settings are same as for Fig. 4. To signify energy savings, we focus on the required SNR for each value of interference-to-signal ratio (σ_2^2/σ_1^2) to achieve the desired QoS, i.e. FER of 10^{-2}. It shows that when the interference x_2 has a lower rate as compared to the desired stream x_1, the required SNR of x_1 for meeting the required QoS decreases with the increase of interference strength which can be attributed to the partial decoding of interference by the MF based receiver. So the BSs need to transmit with lower power if there is lower rate interference in the system as compared to the case when higher rate interference is present in the system.

For the system level perspective, we consider a simple example of two neighboring cells using the proposed FFR strategy thereby doubling the spectral efficiency for *far* (cell-edge) users [32]. These users will be subsequently facing one dominant interference from the neighboring cell. We focus on the two cell edge users in each cell, one out of which is a high data rate user while the other is a low data rate user. To demonstrate the energy efficiency of exploiting the lower rate interference, we consider two ways of subcarriers assignment. In one way which we call as *uniform allocation*, same group of subcarriers in both the cells is used to serve high data rate users while another group is allocated to low data rate users. In this case, users in each cell see interference of nearly the same modulation order as the desired stream so users will not be able to effectively exploit this equivalent rate interference. In the second way of subcarriers assignment which we call as *nonuniform allocation*, the group of subcarriers allocated to the high data rate users in one cell will be allocated to the low data rate users in the neighboring cell and vice versa. So the users in one cell will see lower rate interference and will be able to effectively exploit this interference while the users in the other cell will see interference from higher rate and will not be able to effectively exploit this interference. Table. I demonstrates the energy efficiency of *nonuniform allocation* with reference to *uniform allocation* for the above mentioned scenario. The power indicated is the sum power of both the cells required to achieve the FER of 10^{-2} for the users. The energy efficiency of *nonuniform allocation* decreases as the difference between the rates of two streams decreases which can be attributed to the reduction in the ability of exploiting the interference structure. Note that as the coding rate is fixed to $1/2$, so the user rates correspond to fixed modulation order, i.e. 3bps/Hz, 2bps/Hz and 1bps/Hz correspond to 64QAM, 16QAM and QPSK respectively.

The proposed FFR can also be extended to the satellite communications via spot beams where different antenna groups on a satellite have different non-overlapping coverage areas. The idea of effective exploitation of the lower rate/modulation order interference can also be stretched to cellular networks with the frequency reuse of one or to the soft frequency reuse. In cellular scenario, *near* users enjoying a higher SNR have higher rates/modulation orders as compared to the *far* users

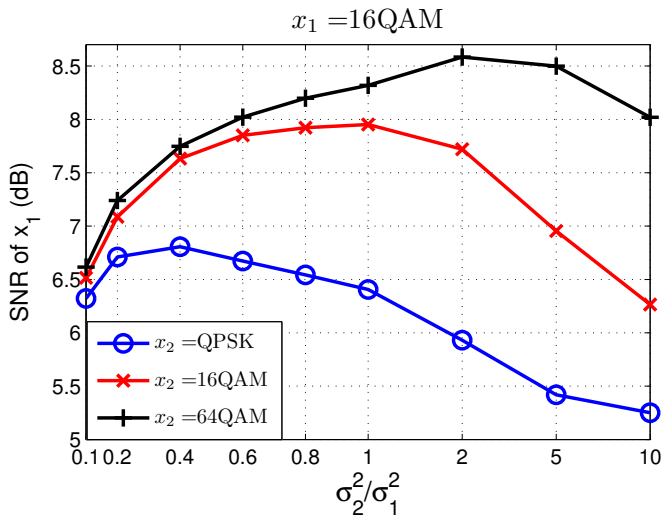

Fig. 8. It shows the required SNR for the desired stream x_1=16QAM for different constellations of interference x_2 for the target FER of 10^{-2}. LTE turbo code (rate $1/2$) is used with maximum of 5 decoding iterations using max log MAP decoder.

suffering from the path loss. Allotment of the same frequency subbands to the near users of one cell as the frequency subbands allocated to the far users of the neighboring cell shall enable higher rate users to exploit the lower rate interferences.

VIII. Conclusions

We have focused in this paper on the scenario of interference suppression and have proposed a low complexity MF based receiver which exploits the structure of interference in mitigating its effects. We have studied the effects of the strength and the modulation order of interference on the performance of the MF based receiver and linear MMSE receiver and have shown that where MMSE detection loses one order of diversity, the MF based receiver recuperates this lost diversity order. Moreover as the interference gets stronger, the MF based receiver has a coding gain whereas MMSE receiver suffers from a coding loss. We have further shown that where MMSE detection is independent of the modulation order of interference stream, the MF based receiver benefits from a coding gain as the modulation order or rate of interference trims down. In addition we have also considered the effect of correlation on these receivers. Degrading effect of the correlation is less pronounced for the MF based receiver as compared to MMSE receiver especially in the cases when interference because of its relative rate or strength allows its partial decoding. The idea of effective exploitation of lower rate interference by low complexity MF based receiver led to the proposition of a novel FFR scheme which is both spectrally and energy efficient than state of the art FFR scheme.

Appendix A
Derivation of PEP of low complexity MF based receiver

As the proposed MF based receiver is a low complexity version of the max log MAP receiver, so the conditional PEP between correct codeword $\underline{\mathbf{c}}_1$ and error codeword $\hat{\underline{\mathbf{c}}}_1$, i.e. $P\left(\underline{\mathbf{c}}_1 \rightarrow \hat{\underline{\mathbf{c}}}_1|\overline{\overline{\mathbf{H}}}\right) = \mathcal{P}^{\hat{\underline{\mathbf{c}}}_1}_{\underline{\mathbf{c}}_1|\overline{\overline{\mathbf{H}}}}$ is given as [33]

$$\mathcal{P}^{\hat{\underline{\mathbf{c}}}_1}_{\underline{\mathbf{c}}_1|\overline{\overline{\mathbf{H}}}} = P\left(\sum_{k'} \min_{x_1\in\chi^i_{1,c_{k'}},x_2\in\chi_2} \frac{1}{N_0}\left\|\mathbf{y}_k - \mathbf{h}_{1,k}x_1 - \mathbf{h}_{2,k}x_2\right\|^2 \geq \sum_{k'} \min_{x_1\in\chi^i_{1,\hat{c}_{k'}},x_2\in\chi_2} \frac{1}{N_0}\left\|\mathbf{y}_k - \mathbf{h}_{1,k}x_1 - \mathbf{h}_{2,k}x_2\right\|^2\right) \tag{11}$$

where $\overline{\overline{\mathbf{H}}} = [\mathbf{H}_1 \cdots \mathbf{H}_N]$ is the channel for the transmission of codeword $\underline{\mathbf{c}}_1$. Assume $d\left(\underline{\mathbf{c}}_1 - \hat{\underline{\mathbf{c}}}_1\right) = d_{free}$ for $\underline{\mathbf{c}}_1$ and $\hat{\underline{\mathbf{c}}}_1$ under consideration for PEP analysis, which is the worst case scenario between any two codewords as d_{free} is the minimum Hamming distance of the code. Therefore, inequality on the right hand side of (11) shares the same terms on all but d_{free} summation points for which $\hat{c}_{k'} = \bar{c}_{k'}$ where $(\bar{.})$ denotes the binary complement. Let

$$\begin{aligned}\tilde{x}_{1,k}, \tilde{x}_{2,k} &= \arg \min_{x_1\in\chi^i_{1,c_{k'}},x_2\in\chi_2} \frac{1}{N_0}\left\|\mathbf{y}_k - \mathbf{h}_{1,k}x_1 - \mathbf{h}_{2,k}x_2\right\|^2 \\ \hat{x}_{1,k}, \hat{x}_{2,k} &= \arg \min_{x_1\in\chi^i_{1,\bar{c}_{k'}},x_2\in\chi_2} \frac{1}{N_0}\left\|\mathbf{y}_k - \mathbf{h}_{1,k}x_1 - \mathbf{h}_{2,k}x_2\right\|^2\end{aligned} \tag{12}$$

As $x_{1,k}$ and $x_{2,k}$ are the transmitted symbols so $\left\|\mathbf{y}_k - \mathbf{h}_{1,k}x_{1,k} - \mathbf{h}_{2,k}x_{2,k}\right\|^2 \geq \left\|\mathbf{y}_k - \mathbf{h}_{1,k}\tilde{x}_{1,k} - \mathbf{h}_{2,k}\tilde{x}_{2,k}\right\|^2$. The conditional PEP is given as

$$\begin{aligned}\mathcal{P}^{\hat{\underline{\mathbf{c}}}_1}_{\underline{\mathbf{c}}_1|\overline{\overline{\mathbf{H}}}} &\leq Q\left(\sqrt{\sum_{k,d_{free}} \frac{1}{2N_0}\left\|\mathbf{H}_k\left(\hat{\mathbf{x}}_k - \mathbf{x}_k\right)\right\|^2}\right) \\ &= Q\left(\sqrt{\frac{1}{2N_0}\mathrm{vec}\left(\overline{\mathbf{H}}^\dagger\right)^\dagger \boldsymbol{\Delta}\mathrm{vec}\left(\overline{\mathbf{H}}^\dagger\right)}\right)\end{aligned}$$

where $\boldsymbol{\Delta} = \mathbf{I}_{n_r} \otimes \mathbf{D}\mathbf{D}^\dagger$ while $\mathbf{D}_{2K\times K} = \mathrm{diag}\left\{\hat{\mathbf{x}}_1 - \mathbf{x}_1, \hat{\mathbf{x}}_2 - \mathbf{x}_2, \cdots, \hat{\mathbf{x}}_{k,dfree} - \mathbf{x}_{k,d_{free}}\right\}$ where $K = d_{free}$. Note that $\overline{\mathbf{H}} = [\mathbf{H}_1 \cdots \mathbf{H}_K] = \boldsymbol{\Psi}_R^{1/2}[\mathbf{W}_1 \cdots \mathbf{W}_K]\left(\mathbf{I}_K \otimes \boldsymbol{\Psi}_T^{1/2}\right) = \boldsymbol{\Psi}_R^{\frac{1}{2}}\overline{\mathbf{W}}_{n_r\times 2K}\left(\mathbf{I}_K \otimes \boldsymbol{\Psi}_T^{1/2}\right)$. Using the Chernoff bound $Q(x) \leq \frac{1}{2}\exp\left(\frac{-x^2}{2}\right)$ [34] and the Kronecker product identity $\mathrm{vec}(\mathbf{AXB}) = \left(\mathbf{B}^T \otimes \mathbf{A}\right)\mathrm{vec}(\mathbf{X})$ [35], we get

$$\mathcal{P}^{\hat{\underline{\mathbf{c}}}_1}_{\underline{\mathbf{c}}_1|\overline{\overline{\mathbf{H}}}} \leq \frac{1}{2}\exp\left(\frac{-1}{4N_0}\mathrm{vec}\left(\overline{\mathbf{W}}^\dagger\right)^\dagger(\boldsymbol{\Psi}_R)^T \otimes \left(\mathbf{I}_K \otimes \boldsymbol{\Psi}_T^{1/2}\right)\mathbf{D}\mathbf{D}^\dagger\left(\mathbf{I}_K \otimes \boldsymbol{\Psi}_T^{\dagger/2}\right)\mathrm{vec}\left(\overline{\mathbf{W}}^\dagger\right)\right) \tag{13}$$

where we have used the identities $(A\otimes B)^\dagger = A^\dagger \otimes B^\dagger$, $(A\otimes C)(B\otimes D) = AB\otimes CD$ and the relation $\boldsymbol{\Psi}_R^{T/2}\boldsymbol{\Psi}_R^{*/2} = \boldsymbol{\Psi}_R^T$. Using the MGF of Hermitian quadratic form of a Gaussian random variable [36] and proceeding on the lines similar to [37], (13) can be rewritten as

$$\mathcal{P}^{\hat{\underline{\mathbf{c}}}_1}_{\underline{\mathbf{c}}_1} \leq \frac{1}{2\det\left(\mathbf{I} + \frac{1}{4N_0}(\boldsymbol{\Psi}_R)^T \otimes \mathbf{D}\mathbf{D}^\dagger(\mathbf{I}_K \otimes \boldsymbol{\Psi}_T)\right)} \tag{14}$$

which involves the identity, i.e. $\det(\mathbf{I}+\mathbf{A}\otimes\mathbf{BC}) = \det(\mathbf{I}+\mathbf{A}\otimes\mathbf{CB})$, which can be proved as

$$\begin{aligned}\det(\mathbf{I}+\mathbf{A}\otimes\mathbf{BC}) &= \det(\mathbf{I}+(\mathbf{A}\otimes\mathbf{B})(\mathbf{I}\otimes\mathbf{C}))\\ &= \det(\mathbf{I}+\mathbf{A}\otimes\mathbf{CB})\end{aligned}$$

(14) can be further extended as

$$\begin{aligned}\mathcal{P}^{\hat{\underline{\mathbf{c}}}_1}_{\underline{\mathbf{c}}_1} &\overset{(a)}{\leq} \frac{1}{2}\prod_{k=1}^{d_{free}}\prod_{l=1}^{\kappa}\frac{4N_0}{\lambda_l(\mathbf{\Psi}_R)\,\lambda_k\left(\mathbf{D}\mathbf{D}^{\dagger}(\mathbf{I}_K\otimes\mathbf{\Psi}_T)\right)}\\ &\overset{(b)}{=} \frac{1}{2}\prod_{k=1}^{d_{free}}\prod_{l=1}^{\kappa}\frac{4N_0}{\lambda_l(\mathbf{\Psi}_R)\,\theta_k\left\|\hat{\mathbf{x}}_k-\mathbf{x}_k\right\|^2}\end{aligned}$$

In (a) we have first used the identity $\det(\mathbf{I}+\mathbf{A}) = \prod_i(1+\lambda_i(\mathbf{A}))$ which is followed by the identity $\lambda(\mathbf{A}\otimes\mathbf{B}) = \lambda(\mathbf{A})\otimes\lambda(\mathbf{B})$. Note that $\kappa = \text{rank}(\mathbf{\Psi}_R)$. More facts are needed in (a). Let $\mathbf{A}$ is $m\times n$ matrix and $\mathbf{B}$ is $n\times k$ with rank n, then $\text{rank}(\mathbf{AB}) = \text{rank}(\mathbf{A})$ [35]. For (b), we have considered the eigenvalues of $(\mathbf{D}\mathbf{D}^{\dagger})_{2K\times 2K}$, i.e.

$$\lambda_k\left(\mathbf{D}\mathbf{D}^{\dagger}\right) = \begin{cases}\left\|\hat{\mathbf{x}}_k-\mathbf{x}_k\right\|^2 & \text{for}\quad k=1,\cdots,d_{free}\\ 0 & \text{for}\quad k=d_{free}+1,\cdots,2d_{free}\end{cases}$$

Assuming transmit correlation matrix to be full rank, the eigenvalues of $\mathbf{I}_K\otimes\mathbf{\Psi}_T$ in increasing order are

$$\lambda_k(\mathbf{I}_K\otimes\mathbf{\Psi}_T) = \begin{cases}\lambda_1(\mathbf{\Psi}_T) & \text{for}\quad k=1,\cdots,d_{free}\\ \lambda_2(\mathbf{\Psi}_T) & \text{for}\quad k=d_{free}+1,\cdots,2d_{free}\end{cases}$$

Using the lemma 1 of [38], we get

$$\lambda_k\left(\mathbf{D}\mathbf{D}^{\dagger}(\mathbf{I}_K\otimes\mathbf{\Psi}_T)\right) = \theta_k\lambda_k\left(\mathbf{D}\mathbf{D}^{\dagger}\right) \tag{15}$$

so that for each k, there exists a positive real number θ_k such that $\lambda_1(\mathbf{\Psi}_T)\leq\theta_k\leq\lambda_2(\mathbf{\Psi}_T)$. So

$$\lambda_k\left(\mathbf{D}\mathbf{D}^{\dagger}(\mathbf{I}_K\otimes\mathbf{\Psi}_T)\right) = \begin{cases}\theta_k\left\|\hat{\mathbf{x}}_k-\mathbf{x}_k\right\|^2 & \text{for}\quad k=1,\cdots,d_{free}\\ 0 & \text{for}\quad k=d_{free}+1,\cdots,2d_{free}\end{cases}$$

Note that $\left\|\hat{\mathbf{x}}_k-\mathbf{x}_k\right\|^2 \geq d^2_{1,\min}+d^2_{2,\min}$ if $\hat{x}_{2,k}\neq x_{2,k}$ and $\left\|\hat{\mathbf{x}}_k-\mathbf{x}_k\right\|^2 \geq d^2_{1,\min}$ if $\hat{x}_{2,k}=x_{2,k}$. There exists $2^{d_{free}}$ possible vectors of $\left[\hat{x}_{2,1},\cdots,\hat{x}_{2,d_{free}}\right]^T$ based on the binary criteria that $\hat{x}_{2,k}$ is equal or not equal to $x_{2,k}$. We call these events as ξ_i where $i=1,\cdots,2^{d_{free}}$. Consider a particular event ξ_m where amongst d_{free} terms of $\left\|\hat{\mathbf{x}}_k-\mathbf{x}_k\right\|^2$, m terms have $\hat{x}_{2,k}\neq x_{2,k}$. Let the product of θs for these m terms is denoted as $[\theta]^m$ and the product of θs for the remaining $(d_{free}-m)$ terms is denoted as $[\theta]^{m'}$. Conditioned on this event ξ_m, we have

$$\begin{aligned}&\prod_{k=1}^{d_{free}}\prod_{l=1}^{\kappa}\frac{\lambda_l(\mathbf{\Psi}_R)\,\theta_k\left\|\hat{\mathbf{x}}_k-\mathbf{x}_k\right\|^2}{4N_0} \geq \left(\left(d^2_{1,\min}+d^2_{2,\min}\right)^m[\theta]^m\right)^{\kappa}\\ &\times\left(\left(d^2_{1,\min}\right)^{(d_{free}-m)}[\theta]^{m'}\right)^{\kappa}\left(\prod_{l=1}^{\kappa}(\lambda_l(\mathbf{\Psi}_R))^{d_{free}}\right)\left(\frac{1}{4N_0}\right)^{\kappa d_{free}}\end{aligned}$$

So conditional PEP for the correlated case is given as

$$\begin{aligned}\mathcal{P}^{\hat{\underline{\mathbf{c}}}_1}_{\underline{\mathbf{c}}_1|\xi_m} \leq\ & \frac{1}{2}\left(\frac{4N_0}{\sigma_1^2 d^2_{1,\min}}\right)^{\kappa d_{free}}\left(\prod_{l=1}^{\kappa}\frac{1}{(\lambda_l(\mathbf{\Psi}_R))^{d_{free}}}\right)\\ &\times\left(\frac{1}{[\theta]^{d_{free}}}\right)^{\kappa}\frac{1}{\left(1+\frac{d^2_{2,\min}}{d^2_{1,\min}}\right)^{m\kappa}}\end{aligned} \tag{16}$$

where $[\theta]^{d_{free}}$ indicates the product $\theta_1\theta_2\cdots\theta_{d_{free}}$. The probability of this event ξ_m is given as

$$P(\xi_m) = (P(\hat{x}_{2,k}\neq x_{2,k}))^m(1-P(\hat{x}_{2,k}\neq x_{2,k}))^{d_{free}-m}$$

$P(\hat{x}_{2,k}\neq x_{2,k})$ is the uncoded probability that the output of max log MAP receiver $\hat{x}_{2,k}$ is not equal to the actual transmitted symbol $x_{2,k}$ and has been derived in Appendix C. Considering all possible events ξ_is, the PEP is upper bounded as (9) in section V.

Appendix B
PEP Analysis of MMSE receiver

For the performance analysis of MMSE receiver, we consider only receive correlation, i.e. channel matrix is given by $\mathbf{H}_k = \mathbf{\Psi}_R^{1/2}\mathbf{W}_k$. Conditional PEP for MMSE based on the Gaussian assumption of post detection interference is given as

$$\mathcal{P}^{\hat{\underline{\mathbf{c}}}_1}_{\underline{\mathbf{c}}_1|\overline{\mathbf{H}}} = P\left(\sum_{k'}\min_{x_1\in\chi^i_{1,c_{k'}}}\frac{1}{N_k}|y_k-\alpha_k x_1|^2 \geq \sum_{k'}\min_{x_1\in\chi^i_{1,\hat{c}_{k'}}}\frac{1}{N_k}|y_k-\alpha_k x_1|^2\right)$$

Let

$$\tilde{x}_{1,k} = \arg\min_{x_1\in\chi^i_{1,c_{k'}}}\frac{1}{N_k}|y_k-\alpha_k x_1|^2$$

$$\hat{x}_{1,k} = \arg\min_{x_1\in\chi^i_{1,\bar{c}_{k'}}}\frac{1}{N_k}|y_k-\alpha_k x_1|^2$$

Considering the worst case scenario $d(\mathbf{c}_1-\hat{\mathbf{c}}_1) = d_{free}$ and using the fact that $\frac{1}{N_k}|y_k-\alpha_k x_{1,k}|^2 \geq \frac{1}{N_k}|y_k-\alpha_k\tilde{x}_{1,k}|^2$, the conditional PEP is upper bounded as

$$\begin{aligned}\mathcal{P}^{\hat{\underline{\mathbf{c}}}_1}_{\underline{\mathbf{c}}_1|\overline{\mathbf{H}}} &\leq Q\left(\sqrt{\sum_{k,d_{free}}\frac{\alpha_k^2}{2N_k}|\hat{x}_{1,k}-x_{1,k}|^2}\right)\\ &\leq \frac{1}{2}\exp\left(-\frac{d^2_{1,\min}}{4}\sum_{k,d_{free}}\mathbf{h}^{\dagger}_{1,k}\mathbf{R}^{-1}_{2,k}\mathbf{h}_{1,k}\right)\end{aligned}$$

where we have used $\frac{\alpha_k^2}{N_k} = \mathbf{h}^{\dagger}_{1,k}\mathbf{R}^{-1}_{2,k}\mathbf{h}_{1,k}$, $|\hat{x}_{1,k}-x_{1,k}|^2 \geq d^2_{1,\min}$ and the Chernoff bound. Note that

$$\begin{aligned}&\sum_{k,d_{free}}\mathbf{h}^{\dagger}_{1,k}\mathbf{R}^{-1}_{2,k}\mathbf{h}_{1,k} = \left[\mathbf{w}^{\dagger}_{1,1},\cdots,\mathbf{w}^{\dagger}_{1,d_{free}}\right]\left(\mathbf{I}_{d_{free}}\otimes\mathbf{\Psi}_R^{\frac{\dagger}{2}}\right)\\ &\times\text{diag}\left[\mathbf{R}^{-1}_{2,1},\cdots,\mathbf{R}^{-1}_{2,d_{free}}\right]\left(\mathbf{I}_{d_{free}}\otimes\mathbf{\Psi}_R^{\frac{1}{2}}\right)\left[\mathbf{w}^{T}_{1,1},\cdots,\mathbf{w}^{T}_{1,d_{free}}\right]^T\end{aligned}$$

where $\text{diag}\left[\mathbf{R}^{-1}_{2,1},\cdots,\mathbf{R}^{-1}_{2,d_{free}}\right]$ is a block diagonal matrix with $\mathbf{R}^{-1}_{2,j}$ as its blocks. Using the MGF [36], conditional PEP conditioned on $\underline{\mathbf{h}}_2 = \left[\mathbf{h}_{2,1},\cdots,\mathbf{h}_{2,d_{free}}\right]$ is upper bounded as

$$\mathcal{P}^{\hat{\underline{\mathbf{c}}}_1}_{\underline{\mathbf{c}}_1|\underline{\mathbf{h}}_2} \leq \frac{1}{2\prod_{i=1}^{n_r d_{free}}\left(\frac{d^2_{1,\min}}{4}\lambda_i\left(\left(\mathbf{I}_{d_{free}}\otimes\mathbf{\Psi}_R\right)\text{diag}\left[\mathbf{R}^{-1}_{2,1},\cdots,\mathbf{R}^{-1}_{2,d_{free}}\right]\right)\right)}$$

where we have used the identities $\det(\mathbf{I}+\mathbf{AB}) = \det(\mathbf{I}+\mathbf{BA})$, $(\mathbf{A}\otimes\mathbf{B})(\mathbf{C}\otimes\mathbf{D}) = \mathbf{AC}\otimes\mathbf{BD}$ and $\det(\mathbf{I}+\mathbf{A}) = \prod_i(1+\lambda_i(\mathbf{A}))$. We have also assumed that the receive correlation matrix $\mathbf{\Psi}_R$ has full rank. Using the identity that for full rank square matrices $\det(\mathbf{AB}) = \det\mathbf{A}\det\mathbf{B}$ thereby leading to $\prod_i\lambda_i(\mathbf{AB}) = \prod_i\lambda_i(\mathbf{A})\prod_l\lambda_l(\mathbf{B})$, PEP is

further upper bounded as

$$\mathcal{P}^{\hat{\mathbf{c}}_1}_{\mathbf{c}_1|\mathbf{h}_2} \leq \frac{1}{2\left(\frac{d^2_{1,\min}}{4}\right)^{d_{free}n_r}\left(N_0^{-1}\right)^{d_{free}(n_r-1)}} \times \frac{1}{\prod_{i=1}^{n_r}\lambda_i\left(\mathbf{\Psi}_R\right)^{d_{free}}\prod_{l=1}^{d_{free}}\left(\sigma_2^2\|\mathbf{h}_{2,l}\|^2+N_0\right)^{-1}}$$

where we have considered the fact that the eigenvalues of $\mathbf{R}^{-1}_{2,k}$ are

$$\lambda_j\left(\mathbf{R}^{-1}_{2,k}\right) = \begin{cases} \left(\sigma_2^2\|\mathbf{h}_{2,k}\|^2+N_0\right)^{-1}, & j=1 \\ N_0^{-1}, & j=2,\cdots,n_r \end{cases} \quad (17)$$

So the conditional PEP is upper bounded as (10) in section V.

APPENDIX C
$\mathbf{P}(\hat{x}_{2,k} \neq x_{2,k})$

We look at the uncoded probability that interfering symbol $\hat{x}_{2,k}$ being detected by (12) is not equal to the actual transmitted symbol $x_{2,k}$. Considering the definition of $\hat{x}_{2,k}$ in (12), it can be expanded as

$$\hat{x}_{1,k},\hat{x}_{2,k} = \arg\min_{x_1\in\chi^i_{1,\bar{c}_{k'}},x_2\in\chi_2}\frac{1}{N_0}\left\{\|\mathbf{h}_{1,k}\left(x_{1,k}-x_1\right)+\mathbf{z}_k\|^2 + \|\mathbf{h}_{2,k}\left(x_{2,k}-x_2\right)\|^2+2\Big(\left(\mathbf{h}_{1,k}\left(x_{1,k}-x_1\right)+\mathbf{z}_k\right)^\dagger\mathbf{h}_{2,k}\left(x_{2,k}-x_2\right)\Big)_R\right\} \quad (18)$$

Note that first term in (18) is positive and second and third terms will go to zero if $\hat{x}_{2,k}=x_{2,k}$ thereby implying that $\hat{x}_{2,k}$ is not equal to $x_{2,k}$ only if the sum of the second and third term is negative. So this probability $P\left(\hat{x}_{2,k}\neq x_{2,k}|\mathbf{h}_{1,k},\mathbf{h}_{2,k},x_1\right)=\mathcal{P}^{\hat{x_2}}_{x_2|\mathbf{H}_k,x_1}$ is given as

$$\mathcal{P}^{\hat{x_2}}_{x_2|\mathbf{H}_k,x_1} = P\Bigg(-2\Big(\left(\mathbf{h}_{1,k}\left(x_{1,k}-x_1\right)+\mathbf{z}_k\right)^\dagger\mathbf{h}_{2,k}\left(x_{2,k}-x_2\right)\Big)_R \geq \|\mathbf{h}_{2,k}\left(x_{2,k}-x_2\right)\|^2\Bigg) = Q\left(\sqrt{\frac{\|\mathbf{h}_{2,k}\left(x_{2,k}-x_2\right)\|^2}{2N_0}} + \sqrt{\frac{2}{N_0}}\left(\frac{\left(\mathbf{h}_{1,k}\left(x_{1,k}-x_1\right)\right)^\dagger\mathbf{h}_{2,k}\left(x_{2,k}-x_2\right)}{\sqrt{\|\mathbf{h}_{2,k}\left(x_{2,k}-x_2\right)\|^2}}\right)_R\right)$$

Now we use the bound $Q\left(a+b\right)\leq Q\left(a_{min}-|b_{max}|\right)$. First term is minimized by the bound $|x_{2,k}-x_2|^2\geq d^2_{2,\min}$ while the magnitude of second term is $\sqrt{\frac{2}{N_0}}\|\mathbf{h}_{1,k}\|\,|x_{1,k}-x_1|$. For the second term we use the bound $\left(\mathbf{a}^\dagger\hat{\mathbf{b}}\right)_R\leq\|\mathbf{a}\|$ where $\hat{\mathbf{b}}$ is the unit vector. So we get

$$\mathcal{P}^{\hat{x_2}}_{x_2|\mathbf{H}_k} \leq Q\left(\sqrt{\frac{\|\mathbf{h}_{2,k}\|^2 d^2_{2,\min}}{2N_0}}-\sqrt{\frac{2\|\mathbf{h}_{1,k}\|^2 d^2_{1,\max}}{N_0}}\right) \leq \frac{1}{2}\exp\left(-\frac{\|\mathbf{h}_{2,k}\|^2 d^2_{2,\min}}{4N_0}-\frac{\|\mathbf{h}_{1,k}\|^2 d^2_{1,\max}}{N_0} + \frac{\|\mathbf{h}_{2,k}\|\,\|\mathbf{h}_{1,k}\|\,d_{2,\min}d_{1,\max}}{N_0}\right) \quad (19)$$

where we have used the Chernoff bound while $d_{1,\max}$ is the maximum distance of the constellation χ_1. Considering the norms of $\mathbf{h}_{1,k}$ and $\mathbf{h}_{2,k}$, we make two non-overlapping regions as $\left(\|\mathbf{h}_{2,k}\|\geq\|\mathbf{h}_{1,k}\|\right)$ and $\left(\|\mathbf{h}_{2,k}\|<\|\mathbf{h}_{1,k}\|\right)$. Note that in the first region $\|\mathbf{h}_{2,k}\|\|\mathbf{h}_{1,k}\|\leq\|\mathbf{h}_{2,k}\|^2$ while for second region $\|\mathbf{h}_{2,k}\|\|\mathbf{h}_{1,k}\|<\|\mathbf{h}_{1,k}\|^2$. So

$$\mathcal{P}^{\hat{x_2}}_{x_2|\mathbf{H}_k} \leq \frac{1}{2}\Bigg[\exp\left(-\|\mathbf{h}_{2,k}\|^2\frac{d^2_{2,\min}-4d_{2,\min}d_{1,\max}}{4N_0}\right) \times\exp\left(-\frac{\|\mathbf{h}_{1,k}\|^2 d^2_{1,\max}}{N_0}\right)P\left(\|\mathbf{h}_{2,k}\|\geq\|\mathbf{h}_{1,k}\|\Big|\mathbf{h}_{1,k}\right) + \exp\left(-\|\mathbf{h}_{1,k}\|^2\frac{d^2_{1,\max}-d_{2,\min}d_{1,\max}}{N_0}\right) \times\exp\left(-\frac{\|\mathbf{h}_{2,k}\|^2 d^2_{2,\min}}{4N_0}\right)P\left(\|\mathbf{h}_{2,k}\|<\|\mathbf{h}_{1,k}\|\Big|\mathbf{h}_{1,k}\right)\Bigg]$$

We upper bound both the probabilities, i.e. $P\left(\|\mathbf{h}_{2,k}\|\geq\|\mathbf{h}_{1,k}\|\Big|\mathbf{h}_{1,k}\right)$ and $P\left(\|\mathbf{h}_{2,k}\|<\|\mathbf{h}_{1,k}\|\Big|\mathbf{h}_{1,k}\right)$ by 1. Taking expectation over $\mathbf{h}_{2,k}$ conditioned on $\mathbf{h}_{1,k}$ and then subsequently taking expectation over $\mathbf{h}_{1,k}$ yields

$$\mathcal{P}^{\hat{x_2}}_{x_2} \leq \frac{1}{2}\Bigg[\left(\frac{4N_0}{d^2_{2,\min}-4d_{2,\min}d_{1,\max}}\right)^\kappa E_{\mathbf{h}_{1,k}}\exp\left(-\frac{\|\mathbf{h}_{1,k}\|^2 d^2_{1,\max}}{N_0}\right) \times\prod_{l=1}^{\kappa}\frac{1}{\lambda_l\left(\mathbf{\Psi}_R\right)} + \left(\frac{4N_0}{d^2_{2,\min}}\right)^\kappa\prod_{l=1}^{\kappa}\frac{1}{\lambda_l\left(\mathbf{\Psi}_R\right)} \times E_{\mathbf{h}_{1,k}}\exp\left(-\|\mathbf{h}_{1,k}\|^2\frac{d^2_{1,\max}-d_{2,\min}d_{1,\max}}{N_0}\right)\Bigg] \leq \frac{1}{2}\left(\frac{4N_0}{\sigma_2^2\check{d}^2_{2,\min}}\right)^\kappa\left(\frac{N_0}{\sigma_1^2\check{d}^2_{1,\max}}\right)^\kappa\prod_{l=1}^{\kappa}\frac{1}{\left(\lambda_l\left(\mathbf{\Psi}_R\right)\right)^2} \times\left(\frac{1}{\left(1-\frac{4\sigma_1\check{d}_{1,\max}}{\sigma_2\check{d}_{2,\min}}\right)^\kappa}+\frac{1}{\left(1-\frac{\sigma_2\check{d}_{2,\min}}{\sigma_1\check{d}_{1,\max}}\right)^\kappa}\right) \quad (20)$$

where we have used the MGF of Hermitian quadratic form of a Gaussian random variable while writing $\|\mathbf{h}_{j,k}\|^2=\mathbf{h}^\dagger_{j,k}\mathbf{I}_{n_r}\mathbf{h}_{j,k}$ where $\mathbf{h}_{j,k}\sim\mathcal{CN}\left(\mathbf{0},\mathbf{\Psi}_R\right)$. This expression shows the dependence of $P\left(\hat{x}_{2,k}\neq x_{2,k}\right)$ on the interference strength, SNR and the correlation.

REFERENCES

[1] S. Kiani, D. Gesbert, A. Gjendemsjo, and G. Oien, "Distributed power allocation for interfering wireless links based on channel information partitioning," *IEEE Transactions on Wireless Communications*, vol. 8, no. 6, pp. 3004 –3015, June 2009.

[2] A. Zanella, M. Chiani, and M. Win, "MMSE reception and successive interference cancellation for MIMO systems with high spectral efficiency," *IEEE Transactions on Wireless Communications*, vol. 4, no. 3, pp. 1244 – 1253, May 2005.

[3] E. Dahlman, H. Ekstrom, A. Furuskar, Y. Jading, J. Karlsson, M. Lundevall, and S. Parkvall, "The 3G long-term evolution - Radio interface concepts and performance evaluation," in *IEEE 63rd Vehicular Technology Conference VTC-Spring*, vol. 1, May 2006, pp. 137–141.

[4] H. Shen, B. Li, M. Tao, and X. Wang, "MSE-Based Transceiver Designs for the MIMO Interference Channel," *IEEE Transactions on Wireless Communications*, vol. 9, no. 11, pp. 3480 –3489, Nov. 2010.

[5] M. Chiani, M. Win, and H. Shin, "MIMO Networks: The Effects of Interference," *IEEE Transactions on Information Theory*, vol. 56, no. 1, pp. 336 –349, Jan. 2010.

[6] S. Verdu, *Multiuser Detection*. U.K.: Cambridge University Press, 1998.

[7] G. Caire, G. Taricco, and E. Biglieri, "Bit-interleaved coded modulation," *IEEE Transactions on Information Theory*, vol. 44, no. 3, pp. 927–946, May 1998.

[8] A. Shah, A. Haimovich, M. Simon, and M.-S. Alouini, "Exact bit-error probability for optimum combining with a Rayleigh fading Gaussian cochannel interferer," *IEEE Transactions on Communications*, vol. 48, no. 6, pp. 908 –912, June 2000.

[9] M. Chiani, M. Win, and A. Zanella, "Error probability for optimum combining of M-ary PSK signals in the presence of interference and noise," *IEEE Transactions on Communications*, vol. 51, no. 11, pp. 1949 – 1957, Nov. 2003.

[10] ——, "On optimum combining of M-PSK signals with unequal-power interferers and noise," *IEEE Transactions on Communications*, vol. 53, no. 1, pp. 44 – 47, Jan. 2005.

[11] N. Kim, Y. Lee, and H. Park, "Performance Analysis of MIMO System with Linear MMSE Receiver," *IEEE Transactions on Wireless Communications*, vol. 7, no. 11, pp. 4474 –4478, Nov. 2008.

[12] G. J. Foschini and M. J. Gans, "On limits of wireless communication in a fading environment when using multiple antennas," *Wireless Personal Communications*, vol. 6, no. 3, pp. 311–335, March 1998.

[13] LTE, *Evolved Universal Terrestrial Radio Access (E-UTRA); Physical Channels and Modulation, Release 8, V.8.6.0*. 3GPP TS 36.211, 2009.

[14] LTE-A, *Evolved Universal Terrestrial Radio Access (E-UTRA); Physical Channels and Modulation, Release 10, V.10.1.0*. 3GPP TS 36.211, 2011.

[15] V. S. Annapureddy and V. V. Veeravalli, "Gaussian interference networks: Sum capacity in the low interference regime and new outer bounds on the capacity region," *IEEE Transactions on Information Theory*, vol. 55, no. 7, pp. 3032 – 3050, July 2009.

[16] C. Oestges, "Validity of the kronecker model for MIMO correlated channels," in *IEEE 63rd Vehicular Technology Conference, VTC-Spring*, vol. 6, May 2006, pp. 2818 – 2822.

[17] H. Shin, M. Win, J. Lee, and M. Chiani, "On the capacity of doubly correlated MIMO channels," *IEEE Transactions on Wireless Communications*, vol. 5, no. 8, pp. 2253 –2265, August 2006.

[18] H. Shin, M. Win, and M. Chiani, "Asymptotic statistics of mutual information for doubly correlated MIMO channels," *IEEE Transactions on Wireless Communications*, vol. 7, no. 2, pp. 562 –573, Feb. 2008.

[19] C.-N. Chuah, D. Tse, J. Kahn, and R. Valenzuela, "Capacity scaling in MIMO wireless systems under correlated fading ," *IEEE Transactions on Information Theory*, vol. 48, no. 3, pp. 637 –650, March 2002.

[20] H. Shin and M. Win, "MIMO Diversity in the Presence of Double Scattering," *IEEE Transactions on Information Theory*, vol. 54, no. 7, pp. 2976 –2996, July 2008.

[21] ——, "Gallager's exponent for MIMO channels: a reliability-rate tradeoff," *IEEE Transactions on Communications*, vol. 57, no. 4, pp. 972 –985, April 2009.

[22] S. Loyka, "Channel capacity of MIMO architecture using the exponential correlation matrix," *IEEE Communications Letters*, vol. 5, no. 9, pp. 369–371, Sep. 2001.

[23] T. M. Cover and J. A. Thomas, *Elements of Information Theory*. New Jersy, USA: John Wiley & Sons, 2006.

[24] R. Ghaffar and R. Knopp, "Interference Suppression for Next Generation Wireless Systems," in *IEEE 69-th Vehicular Technology Conference VTC-Spring 2009*, Barcelona, April 2009.

[25] H. Poor and S. Verdu, "Probability of error in MMSE multiuser detection," *IEEE Transactions on Information Theory*, vol. 43, no. 3, pp. 858–871, May 1997.

[26] R. Ghaffar and R. Knopp, "Spatial Interference Cancellation and Pairwise Error Probability Analysis," in *IEEE International Conference on Communications, ICC 2009*, Dresden, June 2009.

[27] J. Winters, "Optimum combining in digital mobile radio with cochannel interference," *IEEE Journal on Selected Areas in Communications*, vol. 2, no. 4, pp. 528–539, July 1984.

[28] LTE, *Evolved Universal Terrestrial Radio Access (E-UTRA); User Equipment (UE) radio transmission and reception*. 3GPP TS 36.101 Version 10.3.0 Release 10, June 2011.

[29] T. Han and K. Kobayashi, "A new achievable rate region for the interference channel," *IEEE Transactions on Information Theory*, vol. 27, no. 1, pp. 49–60, Jan. 1981.

[30] LTE-A, *Requirements for Further Advancements for Evolved Universal Terrestrial Radio Access (EUTRA) (LTE-Advanced)*. 3GPP TR 36.913, 2008.

[31] FFR, *Interference mitigation : considerations and results on frequency reuse*. 3GPP, TSG-RAN R1-050738,, Siemens, Sept. 2005.

[32] R. Ghaffar and R. Knopp, "Fractional frequency reuse and interference suppression for OFDMA networks," in *8th Intl. Symposium on Modeling and Optimization in Mobile, Ad Hoc, and Wireless Networks (WiOpt 2010)*, Avignon, May-June 2010.

[33] E. Akay and E. Ayanoglu, "Achieving Full Frequency and Space Diversity in Wireless Systems via BICM, OFDM, STBC, and Viterbi Decoding," *IEEE Transactions on Communications*, vol. 54, no. 12, pp. 2164 – 2172, Dec. 2006.

[34] D. Tse and P. Viswanath, *Fundamentals of Wireless Communication*. U.K: Cambridge University Press, 2005.

[35] R. A. Horn and C. R. Johnson, *Matrix Analysis*. Cambridge University Press, U.K, 1985.

[36] G. L. Turin, "The characteristic function of Hermi-

tian quadratic forms in complex normal variables," in *Biometrika*, 1960, pp. 199–201.

[37] A. Hedayat, H. Shah, and A. Nosratinia, "Analysis of space-time coding in correlated fading channels," *IEEE Transactions on Wireless Communications*, vol. 4, no. 6, pp. 2882–2891, 2005.

[38] H. Bolcskei and A. J. Paulraj, "Performance of spacetime codes in the presence of spatial fading correlation," in *Asilomar Conference on Signals, Systems and Computers, 2000*, Pacific Grove, CA, Oct. 2000, pp. 687–693.

Rizwan Ghaffar (S'07-M'10) received the degree of bachelors of electrical (telecommunication) engineering from the National University of Sciences and Technology, Pakistan in 2004. He obtained the M.S. degree in Signals and Digital Communications from Université de Nice - Sophia Antipolis, France in 2007. He received the Ph.D degree in Wireless Communications from Télécom ParisTech, France, in 2010. During 2011, he worked as a researcher in Wireless Telecommunications Laboratory, University of Patras, Greece. He did postdoctoral fellowship in Mobile Communications Department, EURECOM, Sophia Antipolis, France where he worked on EURECOM real-time open-source experimental platform OpenAirInterface.org. Presently he is working as a postdoctoral fellow in University of Waterloo, Canada. R. Ghaffar is the executive editor of European Transactions on Telecommunications. He won the Best Paper Award for the 2011 European Wireless Conference. His current research interests include low complexity receiver design, interference mitigation, single-user MIMO and multi-user MIMO communication systems.

Raymond Knopp was born in Montreal, Canada. He received the B.Eng. (Honours) and the M.Eng. degrees in electrical engineering from McGill University, Montreal, Canada, in 1992 and 1993, respectively. In 1997, he received the PhD degree in communication systems from the Swiss Federal Institute of Technology, Lausanne. During his PhD studies (1993-1997), he was a Research and Teaching Assistant in the Mobile Communications Department of Institut Eurecom, Sophia Antipolis, France. From 1997-2000 he was a research associate in the Mobile Communications Laboratory (LCM-EPFL) of the Communication Systems Department of the Swiss Federal Institute of Technology (EPFL), Lausanne. In 2000 he rejoined the Mobile Communications Department of Institut Eurecom as a Professor.

His current research and teaching interests are in the area of digital communications, software radio architectures, and implementation aspects of signal processing systems. He has published numerous journal and conference articles in these areas. He has participated in collaborative research projects related to wireless communications in the FP5, FP6 and FP7 framework programs as well as French National programs. He is technical coordinator of the OpenAirInterface.org wireless radio platform initiative. These platforms are used in a variety of collaborative research projects and one-to-one projects with both industrial and academic partners to highlight innovative research ideas in wireless networks through experimentation.